Civil Engineering Dimension
https://ced.petra.ac.id

# Assessment and Strengthening of Bolted Connections in the Mandomai Bowstring Bridge Constructed with Ulin Wood

**Subchan, S.K.[1], Awaludin, A.[1]*, Akbar, M.K.[1], Tama, R.G.[1], Setiawan, A.F.[1], Yudhistira, A.T.[1], Irawati, I.S.[1], and Triwiyono, A.[1]**
[1] Department of Civil and Environmental Engineering, Universitas Gadjah Mada, Yogyakarta, INDONESIA

DOI: https://doi.org/10.9744/ced.28.1.101-110

***Article Info:***
Submitted: May 27, 2025
Reviewed: July 07, 2025
Accepted: Aug 12, 2025

***Keywords***:
Bolted connection,
Mandomai,
pedestrian bridge,
retrofit design,
structural testing,
Ulin wood.

***Corresponding Author:***
**Awaludin, A.**
Department of Civil and Environmental Engineering, Universitas Gadjah Mada, Yogyakarta, INDONESIA
Email: ali.awaludin@ugm.ac.id

## Abstract

This study assessed and proposed a retrofit strategy for bolted timber connections in the Mandomai pedestrian bridge, constructed from Ulin wood (*Eusideroxylon zwageri*). Numerical modeling, analytical evaluation using Eurocode 5 yield equations, and experimental validation were conducted. Axial forces from a global Midas Civil model under a 1.25 kN/m² live load showed three critical connections (S11, S13, S14) with demand-capacity ratios (DCR) exceeding 1.0. A retrofit using steel side plates and ASTM A325 bolts reduced DCRs to 0.79, 1.02, and 0.70, respectively. Experimental testing of limited full-scale double-shear wood-to-wood joints demonstrated an average ultimate capacity of 191 kN, which was 57.65% higher than the theoretical prediction, indicating the conservative nature of Eurocode 5 and the contribution of mechanisms such as the rope effect and frictional interlock. The results confirmed the retrofit's effectiveness and highlighted the need to refine design provisions for dense tropical hardwoods.



## INTRODUCTION

The Mandomai pedestrian bridge, located in Central Kalimantan, was designed and constructed between 1973 and 1976 by Swiss structural engineer Heinz Frick in collaboration with students from the Mandomai Vocational School [1]. It was part of a regional effort that involved the construction of three identical bowstring-type timber bridges located in Pulang Pisau, Kuala Kapuas, and Mandomai, using Ulin wood as the primary material. Among the three, only the Mandomai Bridge retained its original timber structure, while the other two were later reconstructed using steel. Since its commissioning in 1976, the Mandomai Bridge served as vital infrastructure, supporting community mobility and transportation. However, in 2021, it was dismantled due to structural component failure and material degradation. One of the key contributing factors to the failure was the inadequacy of the bolted joints, which did not comply with the geometric requirements specified in the National Design Specification (NDS) [2]. Field inspection revealed that several joints failed to meet the minimum spacing requirements: an end distance of 5D, an edge distance of 1.5D, a spacing between bolts in the same row of 4D, and an inter-row spacing of 1.5D. These deficiencies were primarily attributed to the limited timber face height of the members, which ranged only from 180 mm to 220 mm, making it impossible to accommodate compliant bolt configurations. Such geometric constraints likely led to non-uniform stress distribution, joint overstressing, and brittle failure in multiple structural elements. The design of the Mandomai Bridge is shown in Figure 1.

In 2024–2025, the Mandomai Bridge was reconstructed while preserving its original material identity, using Ulin wood (*Eusideroxylon zwageri*), a dense tropical hardwood known for its excellent compressive and bending strength, as well as its natural resistance to weathering and biological degradation [4]. Nevertheless, the structural failure of the previous bridge highlighted the importance of reassessing the joint design in the reconstruction. The geometric

**Note** : Discussion is expected before July, 1st 2026, and will be published in the "Civil Engineering Dimension", volume 28, number 2, September 2026.
**ISSN** : 1410-9530 print / 1979-570X online
**Published by** : **Petra Christian University**

limitation in the timber face remained unchanged, necessitating a careful evaluation of the new bolted connection layout to ensure structural adequacy. Moreover, existing theoretical models such as the yield limit equations in Eurocode 5 are recognized as conservative and may not fully capture the actual mechanical behavior of dense hardwood connections. For this reason, a comprehensive structural assessment and validation process was deemed essential to ensure the safety, reliability, and code compliance of the redesigned bridge structure.

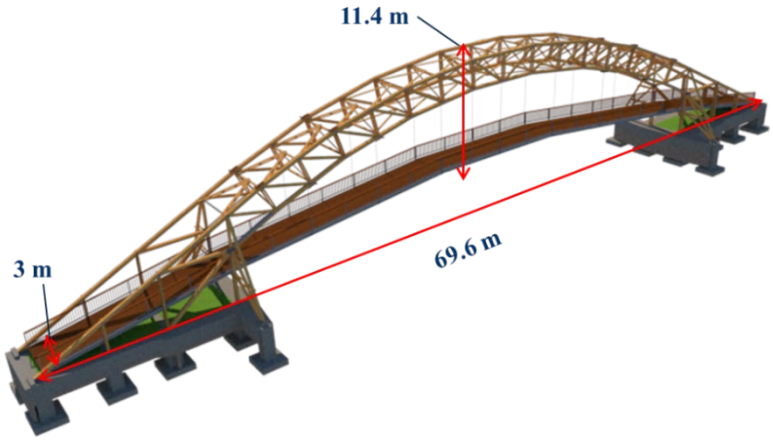


**Figure 1.** Design of Mandomai Bridge [3]

This study aims to evaluate the structural capacity and safety of the bolted joints in the Mandomai Bridge and to propose a strengthening strategy based on both analytical modeling and experimental validation. Axial forces acting on each joint were derived from global structural analysis using Midas Civil software. These internal forces were then assessed relative to the theoretical joint capacities calculated using Eurocode 5 yield limit theory, incorporating appropriate correction factors for geometry and material strength. To validate the theoretical predictions, limited full-scale double-shear tests were conducted on wood-to-wood joint specimens made from Ulin wood. Through this combined analytical and experimental approach, the study seeks to determine the adequacy of current theoretical models in predicting joint performance for tropical hardwood structures with constrained connection geometry, as represented in the Mandomai Bridge case.

## METHODS

### Structural Analysis of Existing Bridge

Structural modeling was conducted to determine the internal axial forces acting on the truss elements of the Mandomai Bridge. These forces were subsequently used to evaluate the loads on each bolted connection. Midas Civil software was employed due to its ability to analyze and manage truss systems, as well as its support for complex structural geometries and various loading combinations. The axial forces obtained from the modeling results served as the basis for calculating the Demand-Capacity Ratio (DCR) at each connection. This DCR was then used in the evaluation of the existing condition and in developing recommendations for structural reinforcement.

The Mandomai Bridge has a total length of 69.6 m, a width of 3.0 m, and an overall structural height of 11.4 m (as shown in Figure 1). It accommodates two pedestrian lanes and two lanes for motorcycles. All structural connections were modeled as bolted connections. The material properties used in the analysis include ASTM A36 steel with a modulus of elasticity of 200 GPa and Ulin wood with a bending modulus of elasticity ($MoE_b$) of 16063 MPa. The density of the Ulin wood is 1070 kg/m³.

Loading conditions were defined in accordance with the Indonesian bridge design standard SNI 1725:2016 [5], encompassing both static and dynamic load combinations to simulate realistic operational scenarios. The static load combination consisted of structural dead load (MS), superimposed dead load (MA), prestressing force from cables (PR), pedestrian live load (TP), and 30% of wind load (EWs), expressed as MA + MS + PR + TP + 0.3 EWs±. Meanwhile, the dynamic combination included motorcycle live loading (MV) in place of pedestrian loading, yielding the expression MA + MS + PR + MV + 0.3 EWs±. These load combinations represent different usage scenarios and were applied to evaluate the impact of various loading patterns on the axial force distribution throughout the structure. The superimposed dead load (MA) accounted for structural components added after the primary structure was

constructed, such as handrails, and was conservatively estimated at 0.5 kN/m. The cable prestressing force (PR) was modeled as a 1 kN pretension force applied to the cables connecting the bridge deck to the truss framework. A uniformly distributed load of 1.25 kN/m² was applied to represent the pedestrian live load. The motorcycle load (MV) was modeled as a moving point load, with rear and front wheel loads of 1.5 kN and 1.7 kN, respectively, and a wheel-to-wheel spacing of 1.4 m [6]. Wind load calculations were performed in accordance with the stipulations of SNI 1725:2016. To reflect actual structural constraints, the model applied boundary conditions consisting of a pinned support at one end and a roller support at the other. The pinned support permitted unrestrained rotation while restraining both vertical and horizontal displacement, whereas the roller support facilitated longitudinal movement. A visual representation of the modeling results is provided in Figure 2.

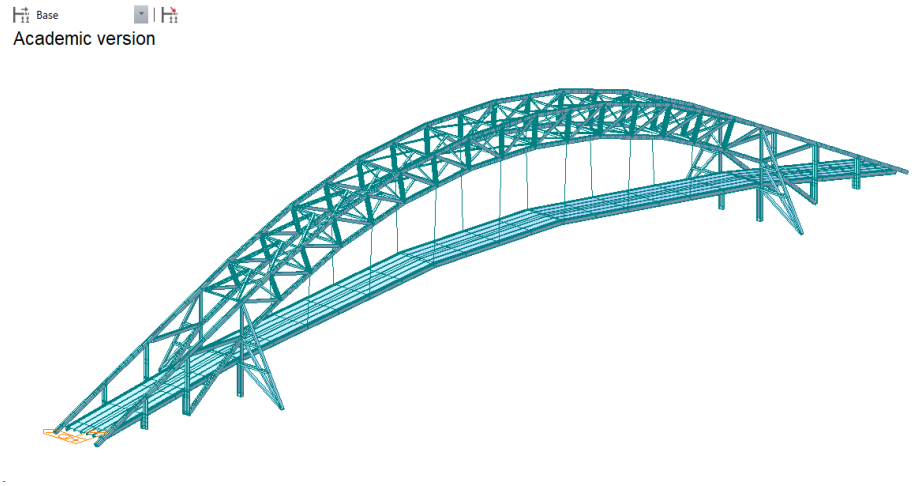


**Figure 2.** Bridge Model in Midas Civil

A linear elastic static analysis was adopted in this model, as the primary objective was to determine axial forces in bridge members under service load conditions. The analysis produced a distribution of axial forces throughout the structure, with notable tensile forces observed in the bottom chords and compressive forces in the top chords. These axial member forces were then mapped to their corresponding joint locations based on the structural configuration of the bowstring truss. The extracted forces served as the basis for evaluating the performance of both the existing and retrofitted bolted joints.

## Connection Design Criteria in Eurocode 5 and NDS

The joint design capacity was calculated using the yield limit theory provided in Eurocode 5, which defines the characteristic load-carrying capacity of dowel-type fasteners based on distinct failure modes. Additionally, the National Design Specification (NDS) employs an approach that focuses on adjusting reference strengths through a series of modification factors to account for service conditions, material variability, and geometric influences. Adjustment factors are applied to adjust the reference strength of wood joints ($F_{v,Rk}$) to account for geometric and material-related conditions affecting joint performance. The corrected joint strength for key fastener types, including bolts, screws, nails, wood screws, dowels, drift bolts, and studs, is calculated using Equation (1).

$$F_{v,Rk}{}' = F_{v,Rk}\, C_D\, C_M\, C_t\, C_g\, C_\Delta\, C_{eg}\, C_{tn} \quad (1)$$

Bolted timber connections are generally categorized into two main types: wood-to-wood (w-t-w) and steel-to-wood (s-t-w) configurations. The load-carrying capacity of each type can be determined using yield limit equations from Eurocode 5, which account for various failure modes depending on the connection geometry and material properties. Figure 3 through Figure 6 illustrate the failure modes associated with double-shear wood-to-wood connections [2], whose capacities are calculated using Equations (2) through (5). Meanwhile, Figure 7 and Figure 8 depict failure modes specific to steel-to-wood double-shear connections [2], corresponding to Equations (6) and (7). A summary of the yield modes along with their corresponding equations is provided in Table 1. The parameters used in these equations include $F_{v,Rk}$, which is the characteristic load-carrying capacity per shear plane per fastener; $f_{h,i,k}$, the characteristic embedment strength of the timber member; $M_{y,Rk}$, the characteristic yield moment of the fastener; and $F_{ax,Rk}$, the characteristic withdrawal resistance of the fastener. Geometrically, $d$ denotes the bolt diameter, $t_1$ refers to the thickness of the outer or side member, and $t_2$ represents the thickness of the inner or main wood member. It should be noted that the resulting capacity from these equations represents the strength of a single shear plane per

bolt, thus, the total joint strength must be calculated by multiplying this value by the number of bolts installed in the connection.

**Table 1.** Yield modes and Their Corresponding Yield Strength

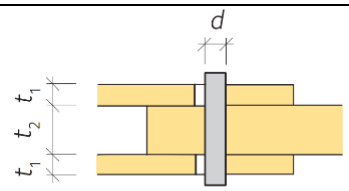


**Figure 3.** Failure Mode $I_s$

$$F_{v,Rk} = f_{h,1,k} t_1 d \quad (2)$$

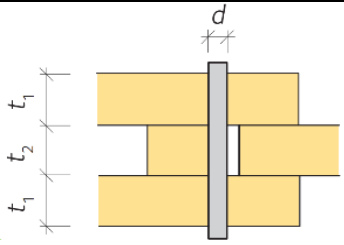


**Figure 4.** Failure Mode $I_m$

$$F_{v,Rk} = 0.5 f_{h,2,k} t_2 d \quad (3)$$

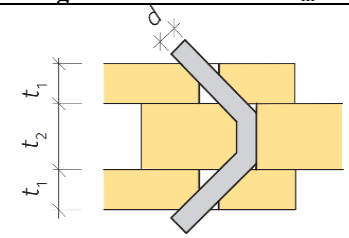


**Figure 5.** Failure Mode $III_s$

$$F_{v,Rk} = 1.05 \frac{f_{h,1,k} t_1 d}{2+\beta} \left( \sqrt{2\beta(1+\beta) + \frac{4\beta(2+\beta) M_{y,Rk}}{f_{h,1,k} d {t_1}^2}} - \beta \right) + \frac{F_{ax,Rk}}{4} \quad (4)$$

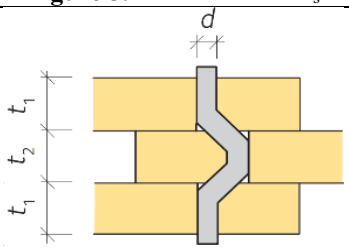


**Figure 6.** Failure Mode IV

$$F_{v,Rk} = 1.15 \sqrt{\frac{2\beta}{1+\beta}} \sqrt{2 M_{y,Rk} f_{h,1,k} d} + \frac{F_{ax,Rk}}{4} \quad (5)$$

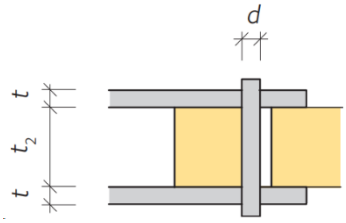


**Figure 7.** Failure Mode I

$$F_{v,Rk} = 0.5 f_{h,2,k} t_2 d \quad (6)$$

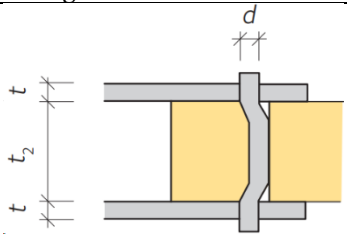


**Figure 8.** Failure Mode II

$$F_{v,Rk} = 1.15 \sqrt{2 M_{y,Rk} f_{h,2,k} d} + \frac{F_{ax,Rk}}{4} \quad (7)$$

## Experimental Wood-to-Wood Connection Testing

Experimental connection tests were carried out for double-shear wood-to-wood to verify the yield limit theory, which states that mechanical fasteners, especially bolts, increase the connection bearing capacity by 25%. The double-shear wood-to-wood testing follows the guidelines of ASTM D5652-95 [7], a standard that outlines the test methods for bolted connections in wood and other wood-based products. This standard serves as a guideline for determining the joint strength values and potential failure modes.

Ulin wood (*Eusideroxylon zwageri*) sourced from the tropical forests of Kalimantan was used as the primary material. The wood type employed is solid (massive) timber without any additional treatment, naturally known for its high resistance to weather and biological degradation. The mechanical properties of Ulin wood, presented in Table 2, were obtained through laboratory testing conducted by Subchan [8,9]. The bolts used have a diameter of M20 with flexural resistance values of $f_y$ 310 MPa and $f_u$ 425 MPa.

**Table 2.** Mechanical Properties of Ulin Wood

| Property | | Strength (MPa) |
|---|---|---|
| Bending modulus of elasticity | $MoE_b$ | 16063 |
| Compressive strength parallel to grain | $fc,_{//}$ | 60.92 |
| Compressive strength perpendicular to grain | $fc,_{\perp}$ | 22.52 |
| Tensile strength parallel to grain | $ft,_{//}$ | 98.53 |
| Shear strength parallel to grain | $fv,_{//}$ | 6.41 |
| Dowel-bearing strength parallel to grain (D20) | $fe,_{//}$ | 56.35 |
| Dowel-bearing strength perpendicular to grain (D20) | $fe,_{\perp}$ | 52.11 |

In this test, the configuration, dimensions, and boundary conditions are shown in Figure 9. Three pieces of Ulin wood, each measuring 65 mm × 130 mm × 500 mm, were connected using M20 bolts. The bolt spacing was designed to meet the minimum standards as specified in NDS regulations.

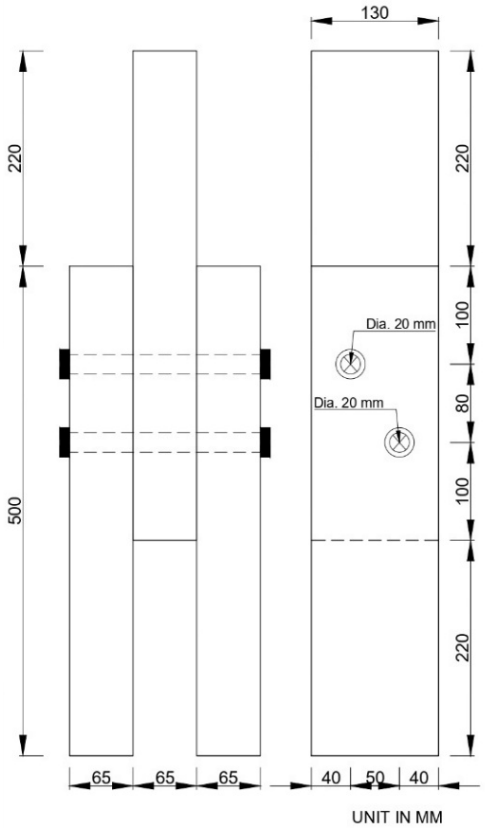


**Figure 9.** Dimensions and Geometry of the Type of Joint

In this experiment, three samples were prepared, each possessing identical characteristics regarding the wood, bolts, and rings, as illustrated in Figure 10(a), ensuring consistency across all specimens to accurately assess the double-shear wood-to-wood connection performance under controlled laboratory conditions.

The experimental procedure involved using a universal testing machine (Figure 10(b)) to apply the load through a hydraulic jack. A load cell with a capacity of 300 kN was used to ensure consistent load application and precise control throughout the testing. The load was estimated based on analytical calculations ($F_{v,Rk}$). Two Linear Variable Differential Transformers (LVDT) with a capacity of 50 mm and a sensitivity of 5.0 mV/V were employed to measure the slip between the middle and side elements. A data logger was used to record all measurements accurately throughout the testing process. The primary parameters observed included the ultimate load, load–displacement response, and failure mode.

(a) (b)

**Figure 10.** (a) Sample Specimen, (b) Experiment Setup

## RESULTS AND DISCUSSION

### Experimental Result

The ultimate loads recorded for Specimens 1, 2, and 3 were 151 kN, 186 kN, and 196 kN, respectively. In Figure 11, specimen 1 exhibited significantly lower strength, with an absolute deviation of 40 kN (over 20%) from the average of Specimens 2 and 3 (191 kN). Visual inspection revealed an irregular surface condition on the underside of Specimen 1, likely contributing to non-uniform stress distribution and premature failure. Based on statistical deviation and mechanical justification [10], specimen 1 was considered an outlier, and further analysis used the average of Specimens 2 and 3.

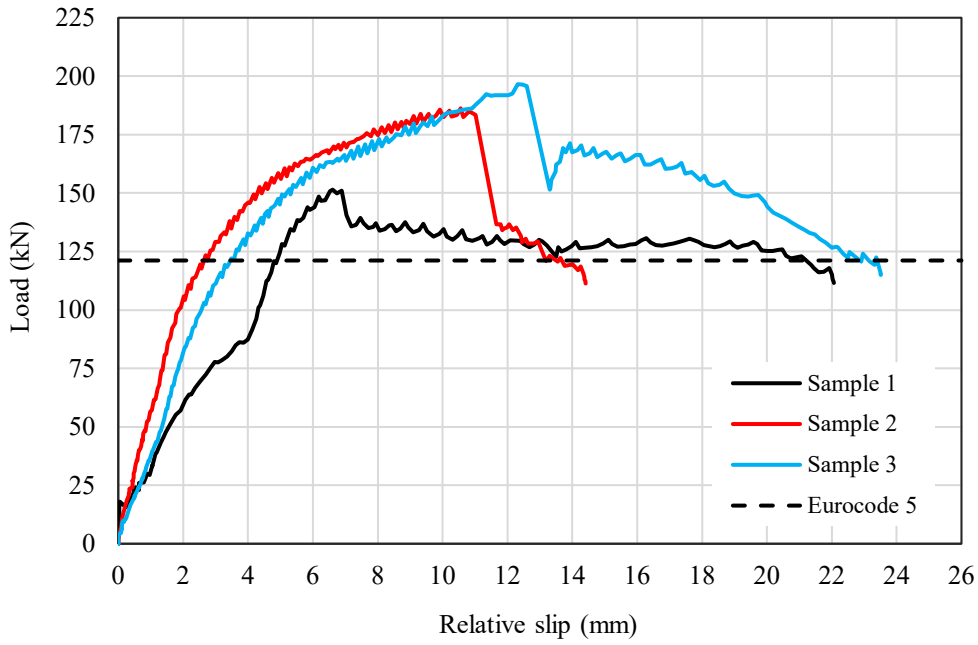


**Figure 11.** Experimental Load-displacement Curve

The test results revealed a significant discrepancy between theoretical predictions and experimental findings. The analytically calculated yield capacity based on Eurocode 5 was 121 kN. In contrast, laboratory testing of the double-shear wood-to-wood joint produced an experimental yield load of 140 kN, as determined using the 5% offset method in accordance with ASTM D5652-95. Furthermore, the ultimate load capacity observed in the test reached 191 kN, indicating a 57.65% increase over the theoretical yield prediction. This substantial surplus suggests the presence of additional resistance mechanisms not considered in the standard yield model, such as rope effect, frictional interlock, or localized densification. Previous studies have reported similar behavior. Debertolis et al. [11] demonstrated that doweled timber joints exhibited an approximate 15% post-yield load increase, despite Eurocode 5 assuming no rope effect contribution for smooth dowels.

The test results indicate that the failure in dowel connections using Ulin wood was predominantly governed by a brittle failure mechanism, visually characterized by damage in the form of embedment and splitting. Embedment failure was evidenced by permanent deformation on the wood surface surrounding the dowel contact area, resulting from localized pressure exceeding the wood's bearing capacity. On the other hand, splitting failure (Figure 12) was observed as longitudinal cracks parallel to the grain direction, particularly in the main joint elements, indicating the presence of transverse tensile stresses due to dowel penetration and uneven force distribution. Based on Eurocode 5 classification, the observed failure corresponds to Mode IV, which involves a combination of dowel yielding and wood crushing or splitting in the main member. These damage characteristics demonstrate the brittle behavior of Ulin wood, which, despite its high compressive strength, tends to fail suddenly without significant deformation when subjected to lateral tensile stress.

**Figure 12.** Wood Failure from the Side

This observation is consistent with the findings of Ji et al. [12], who reported that loading parallel to the grain often leads to abrupt splitting failure once the tensile strength limit is reached. The observed embedment and progressive crushing around washers, as illustrated in Figure 13, corroborate the findings of Domínguez et al. [13]. They demonstrated that combined bending and compressive stresses induced by washers result in increased deformation and altered bearing width. Additional validation comes from Zhou and Zhou [14], who analyzed brittle splitting in dowelled joints under load and reported similar patterns of cracking parallel to the grain.

(a) (b)

**Figure 13.** Failure of Bolts and Inside Wood: (a) Sample 2, (b) Sample 3

## Validation of Eurocode 5 Design Predictions

The experimental results confirmed the conservative nature of the theoretical approach based on Eurocode 5, consistent with observations reported by previous researchers, who have also found that the analytical predictions provided by Eurocode 5 tend to be conservative [15–18]. The experimentally determined average ultimate load of 191 kN exceeded the theoretical prediction by approximately 57.65% than the theoretical yield strength prediction of 121 kN. This substantial discrepancy confirms that the yield limit equations tend to underestimate the actual

strength of bolted wood-to-wood joints, particularly in dense hardwoods such as Ulin. Similar patterns have been reported by Domínguez et al. [13], where experimentally measured strengths substantially exceeded code-based predictions.

Johansen's yield theory includes a rope effect, which allows for up to a 25% increase in joint capacity due to bolt tension and deformation of the surrounding wood. While this enhancement is incorporated into the theoretical model, the observed strength gain in this study surpassed that threshold. This suggests that additional mechanisms, such as increased frictional interlock, localized fiber densification around the dowel, or stress redistribution within the joint zone, may have contributed to the improved resistance beyond what is predicted by design codes [19].

## Connection Analysis of Mandomai Bridge

The connection capacity was determined using the Eurocode 5 yield limit equations, adjusted by service-specific correction factors. These included the wet service factor $C_M$ of 0.85, the group action factor $C_g$ of 0.98, and the geometry factor $C_\Delta$ of 0.90. These coefficients were applied to account for environmental moisture exposure, the distribution of load among multiple fasteners, and the geometric configuration of the joint, respectively. The adjusted values reflect the actual performance conditions of the tropical timber material, ensuring that the predicted capacity remains conservative and safe under design conditions, as formulated in Equation (1). Figure 5 illustrates the joint placement. Based on these calculations, the wood-to-wood connection type failed in Mode IV, while the steel-to-wood connection type failed in Mode II.

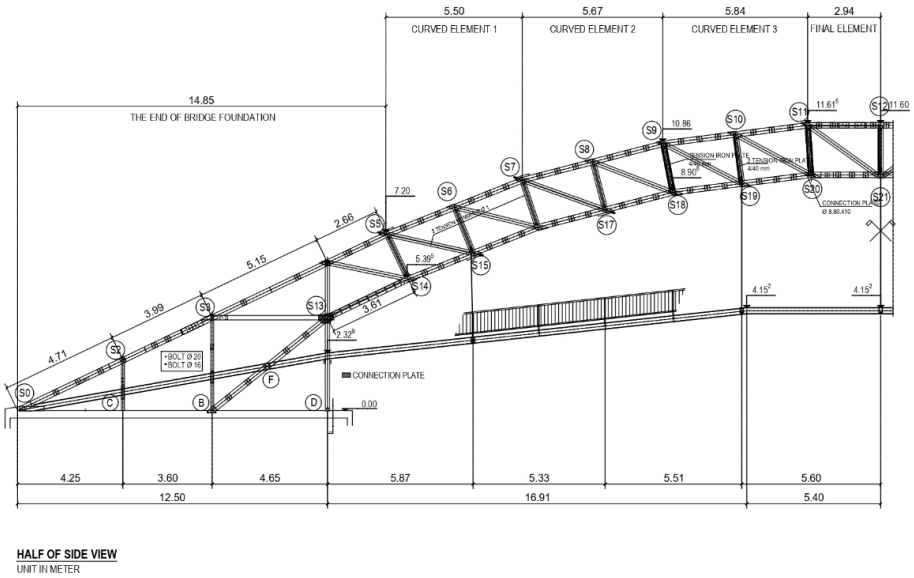


**Figure 14.** Mandomai Bridge's Joint Placement [3]

To assess the structural performance of critical joints in the Mandomai Bridge, a demand-capacity ratio (DCR) analysis was conducted under various design scenarios. The DCR is defined as the ratio between the applied demand (typically an internal force such as axial load) and the available resistance or capacity of the joint. A DCR value greater than 1.0 indicates that the joint is overstressed and potentially unsafe, while values below 1.0 suggest that the joint has sufficient strength to carry the applied loads. In the existing configuration, bolts with a flexural yield strength $f_y$ of 310 MPa and an ultimate strength $f_u$ of 425 MPa were used, resulting in an average bending resistance $f_{yb}$ of 367.5 MPa. Under a design live load of 1.25 kN/m², three joints—S11, S13, and S14—were identified as overstressed, with DCR values of 1.11, 1.52, and 1.40, respectively.

The first retrofitting strategy involved adding side steel plates to joints S11 and S14 to convert them into steel-to-wood configurations, while the bolt material in joints S11 and S13 was upgraded to ASTM A325 high-strength bolts. These bolts provide a yield strength of 660 MPa and an ultimate strength of 830 MPa, resulting in an average $f_{yb}$ of 745 MPa. This intervention significantly reduced the DCR values: S11 dropped to 0.79, S14 to 0.70, while S13 remained slightly above the threshold at 1.02.

Furthermore, when this retrofitting result is considered alongside the laboratory findings, which showed that the experimental ultimate load (191 kN) exceeded the theoretical yield prediction (121 kN) by 57.65%, it further supports

the argument that Eurocode 5 predictions are conservative. Therefore, even though Joint S13 still exhibited a DCR of 1.02 under the 1.25 kN/m² load after bolt strengthening, this condition may still be structurally acceptable when accounting for the additional resistance mechanisms identified in the experimental tests. These include rope effect, bearing densification, and frictional interlock, which are not fully captured in code-based calculations.

## CONCLUSIONS

This study presented a comprehensive structural assessment and retrofit strategy for bolted timber connections in the Mandomai Bridge, constructed from Ulin wood (*Eusideroxylon zwageri*). The investigation combined analytical evaluation using yield limit theory based on Eurocode 5 with full-scale laboratory testing of double-shear wood-to-wood specimens. The structural analysis revealed that three joints (S11, S13, and S14) in the existing bridge exhibited demand-capacity ratios (DCR) greater than 1.0 when subjected to a live load of 1.25 kN/m², indicating overstress conditions. A proposed retrofit strategy consisting of the addition of steel side plates and the application of ASTM A325 high-strength bolts proved effective in reducing all DCRs to below 1.0, except for S13, which slightly exceeded the threshold at 1.02. Experimental validation confirmed that the average ultimate capacity of the joints reached 191 kN, representing a 57.65% increase over the theoretical prediction of 121 kN. This outcome supports the conservative nature of Eurocode 5 and suggests the contribution of additional resistance mechanisms, such as the rope effect, frictional interlock, and localized wood densification, that are not captured in conventional yield limit models. Overall, the findings emphasize that mechanical strengthening, through plate addition and high-strength fasteners, remains the most effective and structurally reliable solution for enhancing the safety and performance of timber joints, especially in hardwood bridges with geometric constraints that limit the flexibility of bolt placement.

## ACKNOWLEDGEMENT

The authors sincerely acknowledge the support from the Department of Civil and Environmental Engineering, Universitas Gadjah Mada, and the financial assistance provided by IAI Central Kalimantan. Appreciation is also extended to the laboratory staff and reviewers for their valuable contributions.

## REFERENCES

1. Dewi, Ar.R.H., Beberapa Pemikiran untuk Rekonstruksi Jembatan Mandomai, *Proceedings of the Seminar Nasional Jembatan Kayu*, 2023.
2. American Wood Council, *National Design Specification (NDS) for Wood Construction*, 2023.
3. Ikatan Arsitektur Indonesia Kalimantan Tengah, *Detail Engineering Design (DED) Jembatan Mandomai*, Palangka Raya, 2024.
4. Brury, U., Baroya, A., Mahdie, M.F., and Thamrin, G.A.R., Uji Ketahanan Kayu Ulin (*Eusideroxylon zwageri*), Bengkirai (*Shorea laevifoia* Endert), dan Meranti Merah (*Shorea leprosula Miq*) sebagai Bahan Baku Pembuatan Perahu terhadap Organisme Perusak Kayu, *Jurnal Sylva Scienteae*, 6(1), 2023, pp. 170-176, https://doi.org/10.20527/JSS.V6I1.8210.
5. Badan Standardisasi Nasional, *SNI 1725:2016 tentang Pembebanan untuk Jembatan*, BSN, Jakarta, Indonesia, 2016.
6. Simanjuntak, J.A.G., *Redesain Jembatan Pejalan Kaki dengan Bahan Cold Formed Steel menggunakan SNI 7971-2013 dan AISI 2002*, Bachelor's thesis, Universitas Gadjah Mada, Yogyakarta, 2021.
7. American Society for Testing and Materials (ASTM), *ASTM D5652-95: Standard Test Methods for Bolted Connections in Wood and Wood-based Products*, 1995.
8. Subchan, S.K., *Analisis Perilaku Struktur Jembatan Pedestrian Tipe Bowstring dari Material Kayu Ulin*, Bachelor's thesis, Universitas Gadjah Mada, Yogyakarta, 2024.
9. Subchan, S.K., *Pengaruh Ketidaksesuaian Persyaratan Geometri terhadap Kekuatan dan Pola Kegagalan Sambungan Baut Kayu Ulin (Studi Kasus: Jembatan Mandomai)*, Master's thesis, Universitas Gadjah Mada, Yogyakarta, 2025.
10. Montgomery, D.C., *Design and Analysis of Experiments*, Ninth Edition., Wiley, 2017, ISBN 9781119589068.
11. Debertolis, M., Wang, Y., Wang, T., Crocetti, R., and Wålinder, M., Rope Effect in Mechanical Panel-Timber Connections: A Comparison between Screws and Dowels, *Engineering Structures*, 332, 2025, https://doi.org/10.1016/J.ENGSTRUCT.2025.120036.
12. Ji, S., Mou, Q., Yuan, G., Ren, H., and Li, X., Dowel–Bearing Behavior of Bamboo Scrimber for Bolted–Type Joint, *Industrial Crops and Products*, 193, 2023, pp. 116178, https://doi.org/10.1016/J.INDCROP.2022.116178.

13. Domínguez, M., Fueyo, J.G., Villarino, A., and Anton, N., Structural Timber Connections with Dowel-Type Fasteners and Nut-Washer Fixings: Mechanical Characterization and Contribution to the Rope Effect, *Materials*, 15(1), 2022, https://doi.org/10.3390/ma15010242.
14. Zhou, H. and Zhou, X., FE Modeling for Bolted Wood Connection using a Porous Constitutive Model, *Advances in Civil Engineering*, 2020, 2020, https://doi.org/10.1155/2020/6621333.
15. Salamah, H., Lee, S.H., and Kang, T.H.K., Investigation of Design Methods in Calculating the Load-Carrying Capacity of Mortise-Tenon Joint of Timber Structure, *Earthquake and Structures*, 25(5), 2023, pp. 307–323, https://doi.org/10.12989/EAS.2023.25.5.307.
16. Quenneville, J.H.P. and Mohammad, M., On the Failure Modes and Strength of Steel-Wood-Steel Bolted Timber Connections Loaded Parallel-to-Grain, *Canadian Journal of Civil Engineering*, 27(4), 2000, pp. 761–773, https://doi.org/10.1139/L00-020.
17. Branco, J.M., Sousa, H.S., and Lourenço, P.B., Experimental Analysis of Maritime Pine and Iroko Single Shear Dowel-Type Connections, *Construction and Building Materials*, 111, 2016, pp. 440–449, https://doi.org/10.1016/J.CONBUILDMAT.2016.02.134.
18. Pošta, J., Hataj, M., Jára, R., Ptáček, P., and Kuklík, P., Comparison of the Use of Angle Brackets in Timber Joints with Eurocode 5, *Construction and Building Materials*, 205, 2019, pp. 611–621, https://doi.org/10.1016/J.CONBUILDMAT.2019.02.053.
19. Lokaj, A., Dobes, P., and Sucharda, O., Effects of Loaded End Distance and Moisture Content on the Behavior of Bolted Connections in Squared and Round Timber Subjected to Tension Parallel to the Grain, *Materials*, 13(23), 2020, pp. 1–21, https://doi.org/10.3390/MA13235525.